Polymer 230 (2021) 124093

Contents lists available at ScienceDirect

Polymer

journal homepage: www.elsevier.com/locate/polymer

Composite polymer hydrogels with high and reversible elongation under magnetic stimuli

F.J. Vazquez-Perez [a], C. Gila-Vilchez [a], J.D.G. Duran [a], A. Zubarev [b,c], L. Alvarez de Cienfuegos [d,e], L. Rodriguez-Arco [a], M.T. Lopez-Lopez [a,e,*]

[a] Universidad de Granada, Departamento de Física Aplicada, Avda. Fuentenueva, 18071, Granada, Spain
[b] Department of Theoretical and Mathematical Physiscs, Ural Federal University, Ekaterinburg, Russia
[c] M N Mikheev Institute of Metal Physics, Ural Branch of the Russian Academy of Science, Ekaterinburg, Russia
[d] Universidad de Granada, Departamento de Química Orgánica, Avda. Fuentenueva, 18071, Granada, Spain
[e] Instituto de Investigación Biosanitaria Ibs.GRANADA, Granada, Spain

ARTICLE INFO

Keywords:
Composite hydrogel
Alginate hydrogel
Soft actuator
Magnetic particles
Microstructural properties
Mechanical behaviour

ABSTRACT

The field of soft actuators is dominated by elastomers that experience mechanical deformations in response to external stimuli. In this context, magnetic stimuli attract considerable interest because of their easy application, tunability, fast response, remote actuation, and safe penetration in biological environments. Since very recently, research interests in the field are being redirected towards hydrogels, which could virtually replace elastomers, overcoming their limitations and expanding the field of application of soft actuators. The mechanical actuation of hydrogels is a nascent field full of challenges, such as achieving reliable and significant responsiveness. Here we demonstrate that the combination of a physical polymer hydrogel with a dispersed phase consisting of clusters of magnetic particles, results in magnetic hydrogel composites that exhibit high and reversible elongation in response to magnetic stimuli. Our analyses show that this response is strongly dependent on the matrix elasticity, the concentration of magnetic particles, and the particle distribution within the network of polymer nanofibres. Our strategy for the maximization of the response of magnetic hydrogels should be a catalyst for the development of novel applications of composite hydrogels, such as a valve remotely actuated by a magnetic field that we also present here as a proof-of-concept.

1. Introduction

Polymer composites able to change their dimensions and shape in response to external stimuli are the base of soft actuators [1–6]. Among the different stimuli, remote magnetic fields represent one of the most attractive ways of actuation due to their ease of use, prompt response and safe penetration in biological environments [7]. Most magnetic actuators found in the literature are based on rigid elastomers, which bend easily under a magnetic field, but present reduced elongation (i.e., normal strain) and negligible swelling in response to it. However, changes in size, especially elongation, of polymer composites are the basis for different applications such as artificial muscles, valves and sensors [42–46]. Most importantly, for *in vivo* biomedical applications, biocompatibility and biodegradability are requirements difficult, if not impossible, to be met by elastomers. For all these reasons, the field of soft actuators is expanded to composite hydrogels, leading to the nascent field of hydrogel machines [8,9]. Hydrogels, especially physical hydrogels, can meet biocompatibility and biodegradability requirements, overcoming the limitations of elastomers, and thus they are already revolutionising fields such as medicine and biomimicry [10–15]. Furthermore, hydrogels, due to their more open and less rigid structure compared to elastomers, can potentially display a wider range of responses to the external stimuli, including swelling and elongation. Nevertheless, because water or biological fluids are the main constituents of hydrogels, the design of magnetic hydrogels with adequate mechanical properties that exhibit significant, reversible and durable actuation in response to an external magnetic field, without destruction of the polymer structure, is still a major challenge, especially when biocompatibility requirements must be met [16]. Some excellent magnetic actuators based on covalently crosslinked hydrogels have been reported to date [7,17–22], whereas the field of magnetic actuators based on physical (non-covalently crosslinked) hydrogels remains

* Corresponding author. Universidad de Granada, Departamento de Física Aplicada, Avda. Fuentenueva, 18071, Granada, Spain.
E-mail address: modesto@ugr.es (M.T. Lopez-Lopez).

https://doi.org/10.1016/j.polymer.2021.124093
Received 27 March 2021; Received in revised form 9 July 2021; Accepted 9 August 2021
Available online 11 August 2021

almost unexplored. Physical hydrogels offer some advantages over chemical hydrogels, such as the absence of chemical crosslinkers that may pose potential toxic hazards, and the reversibility of noncovalent interactions that facilitates injectability and/or self-healing. These advantages of physical hydrogels would make it possible to fabricate biocompatible hydrogel machines that might be injected and actuated by magnetic field after self-healing in the post-injection step.

A precise design at the microscale of the integration of the magnetic particles within the network of polymer nanofibres is required to enable the magnetic actuation of polymer composites [23]. The response of these particles to the magnetic stimulus obviously depends on the macroscopic stiffness of the whole composite, but also on the viscoelasticity of the media at the particle level and the concentration and state of aggregation of the particles, which govern their motion at the microscale. Inside a network of polymer nanofibres, the motion of particles is highly restricted and, thus, the potential changes in dimensions (*e.g.*, elongation) of the magnetic actuators based on them are also limited [24]. Recently we found unexpectedly large changes in the viscoelastic properties of physical magnetic gels, which we attributed to the aggregation of the constituent particles into clusters at the stage of gelation. The particles within the clusters can reply collectively to external magnetic stimuli, enhancing the responsiveness of the physical magnetic gel [25]. Other authors have also demonstrated that a relevant factor influencing the magnetic response of magnetic polymer materials is a predesigned particle distribution, so that particles can collectively respond to the magnetic stimulus. For magnetic elastomers, pre-alignment of the magnetic particles within the polymer matrix proved to be a successful approach to improve their responsiveness to external magnetic fields [26–28] showing higher degree of deformability and even anisotropic mechanical response [29]. Similarly, for magnetic hydrogels based on a chemical network, Sitti's group [7] demonstrated grasping actuation thanks to the pre-established anisotropic distribution of the magnetic particles into chains. However, all these magnetic actuators are based basically on bending and/or twisting, while, to the best of our knowledge, the magnetic field-induced elongation of hydrogels remains almost unexplored in the field of hydrogel actuators, very likely due to the reduced elongation reported in previous works for magnetic hydrogels, and the lack of reversibility [12, 30].

Here we investigate magnetic alginate hydrogels crosslinked by ionic interaction mediated by calcium ions. Our choice of alginate was motivated by its abundance and low cost, as well as by its excellent biocompatibility and biodegradability [31]. With respect to the particular magnetic alginate hydrogels of the present work, we previously evaluated their cytotoxicity *ex vivo* and found that human fibroblasts remained viable after 48 h of cell culture in contact with the hydrogels [32]. We have also evaluated the biocompatibility of other magnetic hydrogels and have not found negative results in terms of *ex vivo* cytotoxicity or damage to vital organs in *in vivo* experiments [33,34]. What is more, some other works have even demonstrated that the presence of magnetic nanoparticles in scaffolds used for tissue engineering applications, stimulates adhesion, proliferation, and differentiation of cells in vitro, and even bone formation *in vivo* [35,36]. In the present work, we first analyse if particle collectivity also enhances the ability of physically crosslinked alginate magnetic hydrogels to elongate in response to external magnetic stimuli. For this, we study the change of length during the process of magnetization under a homogeneous magnetic field (magnetostriction), as the purest balance between elasticity and responsiveness to the applied magnetic field. Our results demonstrate high and reversible magnetostriction for these composite hydrogels, which can be tailored by changing design parameters such as the preparation method, the magnetic particle concentration, or their pre-alignment in a preestablished direction. We then present a theoretical model based on the hypothesis that magnetic particles are aggregated into clusters at the microscale, which provides an accurate description of the experimental results at the macroscale. Finally, we demonstrate that this high and reversible elongation responsiveness to the magnetic field can be exploited in a proof-of-concept valve device.

2. Experimental

2.1. Sample preparation

2.1.1. Alginate-based gels

Alginate-based magnetic gels were prepared by first dispersing sodium alginate (Sigma Aldrich, USA) in distilled water at a concentration of 1 % w/w. Once the solution was clear, 7.5 mg of calcium carbonate ($CaCO_3$, Sigma Aldrich, USA) and 26.7 mg of D-glucono-δ-lactone (GDL, Sigma Aldrich, USA) were mixed with 5 mL of the sodium alginate solution in a plastic vial, and vortexed until full dispersion. When dissolved in water, GDL, hydrolyses to gluconic acid and promotes a slow decomposition of $CaCO_3$ and controlled liberation of Ca^{2+} ions. Each positively charged Ca^{2+} ion is attracted to two alginate chains (negatively charged), acting as crosslinking agent. Therefore, the GDL-mediated change of pH contributed to a homogeneous gelation throughout the hydrogel volume. After 90 min, the gelling mixture was broken up with a vortex mixer until it fully showed a fluid-like behaviour (Fig. S1). Immediately afterwards magnetic particles (silica-coated iron powders Fe-CC, BASF, Germany) were added to the mixture (final concentrations of 2.5, 5 and 7.5 % v/v) and homogenized by 10 min of ultrasonication (AL04-03-230 ultrasonic bath, Advantage Lab, Belgium). Then, we poured the mixture into cylindrical containers and, when additional curing of the hydrogels was sought to increase the stiffness of the matrix (termed as double calcium-cured gels), the same volume of a 45 mM aqueous solution of calcium chloride ($CaCl_2$, Sigma, Aldrich, USA) was added to the mixture. Finally, the containers were left undisturbed overnight to allow complete gelation. To test a potential reinforcement of the specimens by magnetic field-induced alignment of the constituent particles, some of the preparations (termed here as magnetic field-cured gels) were gelled in the presence of an external magnetic field, provided by a coil (magnetic field intensity of 15.7 kA m^{-1}). We investigated three different orientations of the direction of the applied magnetic field with respect to the axis of the cylindrical tubes containing the samples: parallel to the axis, forming an angle of 45° with respect to this axis, and perpendicular to it. Unless otherwise specified, results shown in this work for the magnetic field-cured gels correspond to samples gelled under a magnetic field applied parallel to the axis of the cylindrical containers. The final height and diameter of the obtained cylindrical gel specimens used in magnetostriction experiments were approximately 15 mm and 12 mm, respectively.

Table 1
Identification of the sample types studied in this work.

Sample	Step 1: Curation with $CaCO_3$ for 90 min	Step 2: breakage of the hydrogel and mixture with magnetic particles	Step 3: the samples were left overnight for complete gelation	
			Addition of $CaCl_2$ at the beginning of step 3	Application of a magnetic field during the first hour of step 3
Simple calcium-cured magnetic gel	Yes	Yes	No	No
Double calcium-cured magnetic gel	Yes	Yes	Yes	No
Magnetic field-cured magnetic gel	Yes	Yes	No	Yes

A summary of the conditions used for each preparation is shown in Table 1.

2.1.2. Magnetic suspensions

For the preparation of the magnetic suspensions, we dispersed magnetic particles (Fe-CC, BASF, Germany) with final concentrations of 2.5 %, 5 % and 7.5 % v/v in 5 mL of mineral oil (Alfa Aesar, Germany), followed by sonication for 10 min.

2.1.3. Magnetic elastomers

To prepare the magnetic elastomers, we mixed the magnetic particles (Fe-CC, BASF, Germany) with 5 mL of room-temperature-vulcanizing (RTV) silicone (Gran Velada, Spain) and stirred mechanically. Once the mixture looked homogeneous, we added 0.25 mL (5 % v/v) of the catalyst provided by the manufacturer and stirred to ensure complete mixture. Finally, we poured the mixture into moulds to make cylindrical samples of 20 mm diameter and 1.4 mm height. Samples with three different concentrations of magnetic particles (2.5, 5 and 7.5 % v/v) were prepared.

2.2. Electron microscopy imaging of the iron particles

The morphology (*i.e.*, size and shape) of the iron particles (Fe-CC, BASF, Germany, diameter = 1.5 ± 0.7 μm, see Fig. S2) was characterized by scanning electron microscopy (SEM) by means of a Quanta 3DFEG (FEI, USA) microscope with the accelerating voltage 5/20 kV.

2.3. Scanning electron microscopy imaging of the gel microstructure

The microscopic structure of the hydrogels was analysed by scanning electron microscopy (SEM) using a FEI Quanta 400 microscope (Thermo Fisher Scientific, USA). Specimens were prepared by first fixing the gels in 2.5 % glutaraldehyde solution in cacodylate buffer (0.1 M, pH = 7.4) for 2 h at 4 °C. After this step, the samples were washed with the same buffer (three buffer changes of 15 min each at 4 °C), followed by post-fixation with 1 % osmium tetroxide in dark for 1 h at room temperature. The samples were then washed in distilled water (3 changes every 5 min) and then dehydrated in a gradient of increasing ethanol concentration at room temperature (50 %, 70 %, 90 %, 100 % ethanol, 15 min contact with each phase). Finally, the samples were washed two times more with 100 % ethanol (15 min each time) and desiccated by the critical point method [37] with carbon dioxide in a Leica EM CPD300 dryer (Leica, Germany). The specimens were finally either carbon-coated in a carbon evaporator EMITECH K975X (Fedelco, Spain) or coated with Au–Pd (ion sputtering method) in a Polaron Unit SEM Coating SC7640 sputter coater (Polaron Equipment, United Kingdom).

2.4. Measurement of the Young's modulus of the magnetic gels and elastomers

For the gel samples we measured the Young's modulus under compressive forces, using a rheometer Haake Mars III (Thermo Scientific, Germany) provided with a parallel plate geometry. For this purpose, the sample was placed between the two plates and the variation in height for increasing values of the modulus of the applied normal force was monitored (the upper plate descended at a rate of 0.1 mm s^{-1}). In the case of the elastomer samples, the Young's modulus was evaluated using tensile forces in a DHR-1 rheometer (TA Instruments, USA). All the experiments were conducted at room temperature (25 °C).

The Young's modulus (E) was calculated based on the following equation:

$$\sigma = \frac{F}{S} = E\left|\frac{h(0) - h(F)}{h(0)}\right| \quad (1)$$

Where σ is the normal stress, F is the normal force applied by the plate, S is the sample surface area in contact with the plate, $h(0)$ is the initial height of the sample, and $h(F)$ is the height for each value of the applied force. For each set of experimental conditions, we measured at least three different samples and each sample was tested 4–6 times. Here, we provide the corresponding mean values and standard deviations of the measurements.

2.5. Characterisation of the magnetorheological behaviour

The magnetorheological (MR) behaviour of the ferrogels, the magnetic suspensions and the magnetic elastomers was characterised using a rheometer Physica-Anton Paar MCR 300 (Anton Paar, Germany) equipped with a parallel plate geometry. For the ferrogels and the elastomers we used 20-mm diameter cylindrical specimens with heights of 1 and 1.4 mm, respectively. In the case of the magnetic suspensions, we pipetted enough volume of liquid to cover all the surface of the bottom plate, and then used a 0.3-mm gap thickness ensuring complete contact of the liquid with the top plate. After that, a fixed strain of 0.03 % with frequency equal to 1 Hz was applied for 10 s and the modulus of the complex viscosity was recorded in the absence of field. The field was then turned on and progressively raised in a linear ramp consisting of 30 steps from 0 to 284 kA m^{-1} (field variation in each step = 9.5 kA m^{-1}). For each step of the ramp, the same oscillatory strain was applied, and the modulus of the complex viscosity measured for 10 s. Once the highest field was reached, it was progressively reduced in a linear ramp of 30 steps (field variation in each step = 9.5 kA m^{-1}) and 10 s of duration for each step, with the modulus of the complex viscosity monitored. Once all the measurements under magnetic field application were completed, we re-measured the behaviour in the absence of field. All the samples were measured at room temperature (25 °C).

2.6. Characterisation of the magnetostriction effect

The elongational deformation of magnetic hydrogels under applied magnetic fields up to 57.4 kA m^{-1} (in steps of 7.14 kA m^{-1}) was measured using a CMOS Multi-Function Analogue Laser Sensor (IL series, KEYENCE, Japan), consisting of an IL-S065 sensor head and an IL-1000 amplifier unit. For the application of the magnetic field, we used a coil connected to a DC power supply. The field distribution generated by the coil was simulated by Finite Element Method, using FEMM software, evidencing high homogeneity of the field in the position of the sample (*i.e.*, at centre of the coil), as shown in Fig. S3. The sample height was measured under increasing magnetic fields (with steps of 7.15 kA m^{-1}) until the maximum field (57.4 kA m^{-1}) was reached (upward ramp). To investigate potential hysteresis phenomena, the field was then gradually decreased (downward ramp) while measuring the sample height for each of the fields used in the upward ramp. For each step of the upward or downward ramps, the field was maintained for 1 min, and the sample height was recorded every 5 s. All the measurements were conducted at room temperature. The hysteresis area was quantified from elongation *vs* field intensity plots by subtracting the area under the lower curve (upward ramp) to the area under the upper curve (downward ramp).

In separated experiments, we investigated the fatigue behaviour of hydrogels. For this aim we applied successive cycles consisting of 1 min in the presence of a given value of the applied magnetic field (on state), followed by 1 min in the absence of applied magnetic field (off state). During fatigue experiments we recorded the sample height every 5 s.

2.7. Creep-recovery experiments

Creep-recovery experiments were performed using a Physica-Anton Paar MCR 300 (Anton Paar, Germany) equipped with a parallel plate geometry. With these experiments we sought to estimate the relaxation time of the samples after removal of an applied magnetic field. With this aim, we measured the deformation of the samples during 60 s under a specific stress. The value of the applied stress chosen in each case led to

the same relative deformation obtained in the magnetostriction experiments. After 60 s, the stress was removed, and we monitored again the deformation of the samples for 60 s. We recorded the deformation every 0.1 s, thus obtaining 1200 points per experiment. The samples were prepared in the shape of discs with a diameter of 20 mm and 1 mm of thickness.

2.8. Construction of a valve actuated by the magnetic field

To test the potential applicability of magnetic field-induced changes in dimensions of the gel in actuators, we built a device aimed to work as a valve. The device was printed with a 3D printer XYZ PRINTING Da Vince 1.0A (XYZ PRINTING, USA) and consisted of a main channel (rectangular section, side length = 5 mm, height = 20 mm) provided with a reservoir for the magnetic gel (simple calcium-cured at a concentration of 7.5% v/v of magnetic particles in these experiments). Downstream of the reservoir, the channel was equipped with a lateral input (see Fig. 4a) connected to a supply of fresh water and giving the device an approximate Y shape. A constant supply of an orange dye solution (Orange II sodium salt, concentration 5 gL^{-1}, Sigma-Aldrich) was fed to the main channel, which was initially blocked by the hydrogel. When a neodymium magnet (428 mT at the surface level) was approached to the hydrogel, it contracted perpendicularly to the direction of the flow because of the magnetic field, and allowed the orange dye solution to flow through the main channel, thus leading to an output of orange-coloured liquid. When the magnet was removed, the gel virtually recovered its original dimensions, blocking the channel again. Thanks to the continuous supply of fresh water by the lateral input, the liquid at the outlet of the tube became transparent again.

3. Results and discussion

Three main types of magnetic composites, based on dispersions of magnetic particles, can be identified depending on the viscous and elastic properties of the carrier matrix (Fig. 1a). In this work, we focus on magnetic hydrogels based on an alginate polymer crosslinked by addition of $CaCO_3$, and a dispersed magnetic phase consisting of iron particles (Fig. 1b). For some preparations we also introduced some additional changes in the protocol, either by conducting stronger gelation upon addition of $CaCl_2$ (double calcium-curing), or by the application of a magnetic field for 1 h after particle addition (magnetic field-curing), as illustrated in Fig. 1b (see also Table 1). The Young's modulus

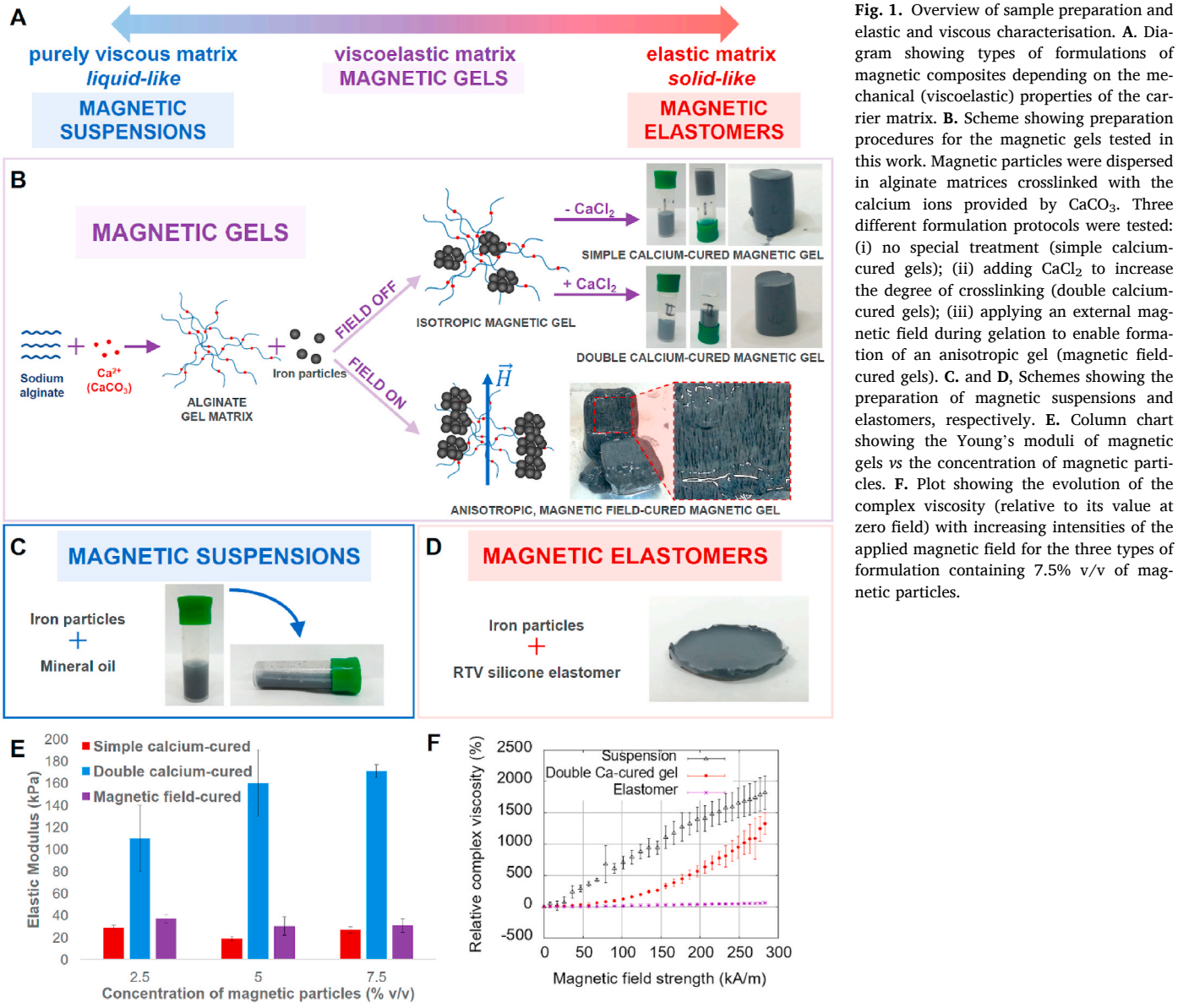

Fig. 1. Overview of sample preparation and elastic and viscous characterisation. **A.** Diagram showing types of formulations of magnetic composites depending on the mechanical (viscoelastic) properties of the carrier matrix. **B.** Scheme showing preparation procedures for the magnetic gels tested in this work. Magnetic particles were dispersed in alginate matrices crosslinked with the calcium ions provided by $CaCO_3$. Three different formulation protocols were tested: (i) no special treatment (simple calcium-cured gels); (ii) adding $CaCl_2$ to increase the degree of crosslinking (double calcium-cured gels); (iii) applying an external magnetic field during gelation to enable formation of an anisotropic gel (magnetic field-cured gels). **C.** and **D**, Schemes showing the preparation of magnetic suspensions and elastomers, respectively. **E.** Column chart showing the Young's moduli of magnetic gels *vs* the concentration of magnetic particles. **F.** Plot showing the evolution of the complex viscosity (relative to its value at zero field) with increasing intensities of the applied magnetic field for the three types of formulation containing 7.5% v/v of magnetic particles.

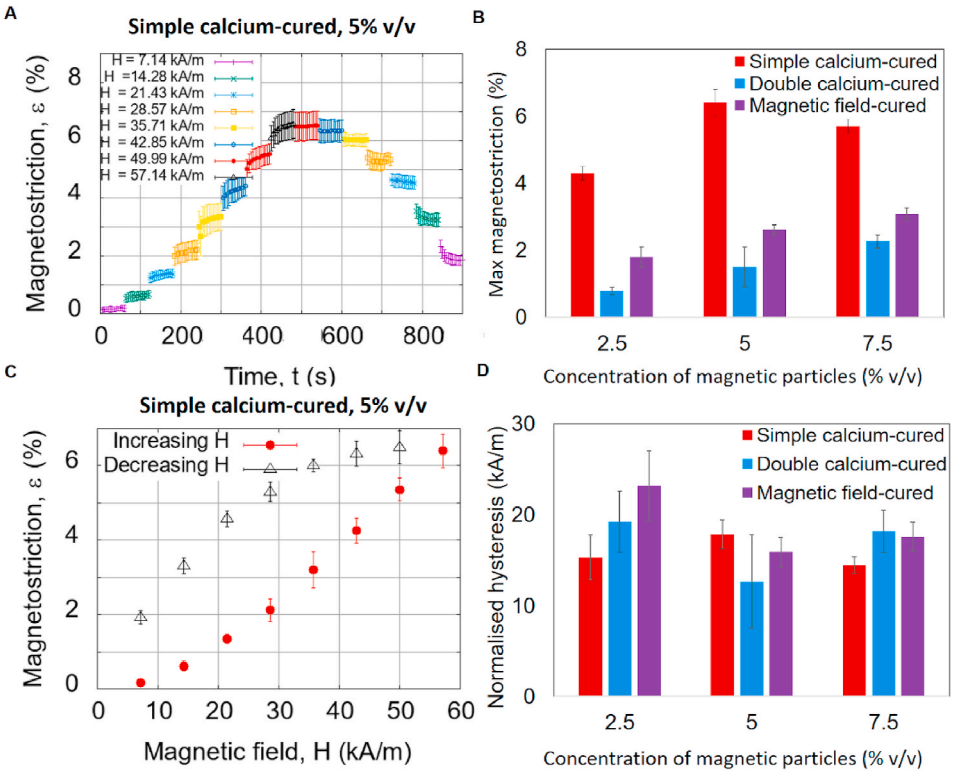

Fig. 2. Magnetostriction of magnetic gels. **A.** Plot showing the time evolution of the magnetostriction, ε (equation (2)), for a simple calcium-cured magnetic gel (5 % v/v iron particle concentration) under magnetic field application. Similar results were obtained for other gel types or particle concentrations (see Fig. S6-S8) **B.** Column chart comparing the maximum magnetostriction (*i.e.*, relative elongation) experienced by all the gel types *vs.* the volume fraction of particles in the gels. **C.** Plot of the magnetostriction values (simple calcium-cured gel, 5 % v/v iron content) as a function of the magnetic field to demonstrate the hysteretic behaviour for gel deformation. Similar results were obtained for other gel types or particle concentrations (see Fig. S6-S8). **D.** Column chart representing the hysteresis area between the upward and downward curves of plots like those in C, normalized by the maximum value of magnetostriction.

strongly increased when the samples were double calcium-cured compared to the samples not subjected to an additional curing step (*i.e.*, simple calcium-cured gels), while no significant increases of this quantity were measured for gels subjected to a magnetic field during curing (see Fig. 1e). Indeed, for the double calcium-cured gels (7.5% v/v) the Young's modulus was of the same order of magnitude as for an elastomer with the same volume fraction of magnetic particles (352 ± 53 kPa). All the magnetic gel preparations were dark grey in colour, associated with the magnetic particles, self-standing, and did not flow when the sample vials were turned upside down (Fig. 1b). For double calcium-cured gels, the samples shrank in the radial direction during the curing step, losing contact with the vial walls and falling to the bottom of the vial when it was turned upside down, due to gravity, but the gel integrity was maintained. In the case of magnetic field-curing, black chain-like aggregates of magnetic particles aligned in the direction of the field could be clearly identified with the naked eye (Fig. 1b). Finally, and for comparison, we also prepared magnetic composites on the other ends of the formulation spectrum, *i.e.*, magnetic suspensions and magnetic elastomers, with the same particle concentrations used for the hydrogels (2.5, 5 and 7.5 % v/v). In the first case, we simply dispersed the magnetic particles in mineral oil (viscosity at 25 °C is 0.028 ± 0.001 Pa s), which led to a liquid-like sample that could be easily poured from the container (Fig. 1c). For the preparation of the elastomers, the magnetic particles were dispersed in room-temperature-vulcanizing (RTV) silicone, resulting in a self-standing, rubber-like disk (Fig. 1d).

We first confirmed that the rheological (*i.e.*, flow) behaviour of the gels under external stresses was intermediate between those of the suspension and the elastomer. To confirm this, we placed the samples between the two parallel plates of a rheometer and allowed the upper plate to rotate to induce a shear stress. At the same time, an external magnetic field was applied in the direction perpendicular to the plates to monitor changes of the sample complex viscosity with the intensity of the magnetic field. As expected, this change was almost negligible for the magnetic elastomer, because of the reduced mobility of the magnetic particles in the crosslinked silicone network, which hindered assembly of chain-like structures (Fig. 1f). On the contrary, the suspension exhibited strong increases of the complex viscosity under an applied magnetic field and started to get saturated at the highest fields (Fig. 1f). Indeed, the liquid-like nature of the mineral oil carrier allowed the magnetic particles to freely move to build aggregates in the field direction, leading to a strong change of the suspension viscosity with the field. The behaviour of the gel (double calcium-cured in Fig. 1f) was in between these two extreme cases. At low magnetic fields, the change of viscosity with the field was weak, like the elastomer case. However, under medium to high fields, the viscosity strongly changed with the field intensity, even at a faster rate than for the suspension at the highest fields (Fig. 1f). This could be explained by the different microscopic structures of the three formulations. In the case of the gel, the elasticity of the alginate network dominates at low fields, while magnetic forces between the constituent particles become dominant as the field increases, which explains why the viscosity of the magnetic gel approached rapidly the typical values for the suspension. However, in the case of the magnetic elastomer, the polymer network is so stiff that its elasticity dominates over magnetic forces even for the highest magnetic fields. Similar trends were obtained for lower particle concentrations (2.5 % v/v and 5 % v/v, see Fig. S4), although the difference in the MR effect between the suspensions and the gels at these lower particle concentrations became considerably larger, even at the highest magnetic fields. This could be explained because at lower particle concentration, the particle clusters were more spatially sparse, and the magnetic interaction between them would have been weaker, consistent with its rapid decay with distance (it scales with r^{-4}, r being the separation distance between magnetic domains under the dipole approximation). As a result, the magnetic interaction was likely not large enough to overcome the elasticity of the alginate network at 2.5 % and 5 % v/v.

Once the flow behaviour upon external stress was characterised, we undertook a series of experiments in the absence of external forces other than the external magnetic field (we corrected the values for the effect of gravity and potential dehydration), intended to investigate the ability of magnetic gels to change their dimensions in response to applied magnetic fields. To quantify this response in such a way that it can be

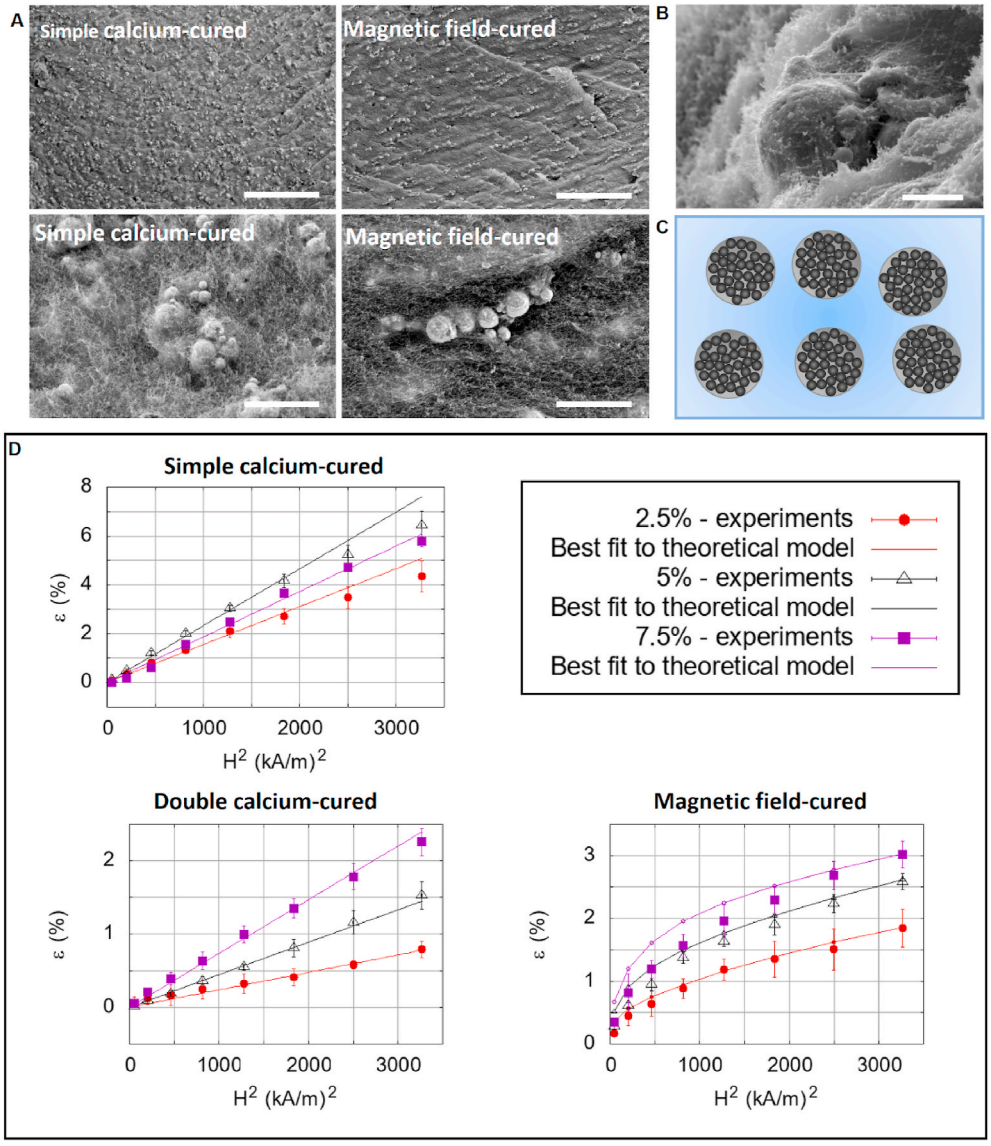

Fig. 3. Particle cluster formation within magnetic gels and theoretical model. **A.** Scanning electron microscopy (SEM) micrographs for the simple calcium-cured and magnetic field-cured gels. Scale bars correspond to 100 μm and 10 μm for the top and bottom images, respectively. **B.** High magnification SEM image of magnetic particles within the alginate network which allows identification of polymeric fibres attached to the surface of the magnetic particles. Scale bar = 2 μm. **C.** Sketch depicting magnetic particle clusters (grey spheres) within an alginate network (blue colour) as considered by our theoretical model. **D.** Plots showing the magnetostriction (as in Fig. 2A) vs. the square of the magnetic field intensity, H^2 for the simple calcium-cured, double calcium-cured and magnetic field-cured gels. Experimental data (symbols) are plotted together with best fits to equation (S8) for the simple calcium-cured and double calcium-cured gels, and to equation (S19) for the magnetic field-cured gels. (For interpretation of the references to colour in this figure legend, the reader is referred to the Web version of this article.)

objectively compared with other systems, we selected magnetostriction, as the purest balance between elasticity and responsiveness to the applied magnetic field. For this aim, we monitored the changes in length of cylinder-like specimens over time and upon increasing magnetic field intensity using a laser sensor. When the field was activated, the gel samples underwent positive magnetostriction, that is, a positive value of the normal strain, ε, under the magnetic field was measured:

$$\varepsilon = \frac{h - h_0}{h_0}, \tag{2}$$

Here h and h_0 are respectively the sample height under a magnetic field H and in the absence of magnetic field. This relative elongation (normal strain ε) progressively increased as the magnetic field intensity was raised, as shown in Fig. 2a for a concentration of particles of 5 % v/v in a simple calcium-cured gel. Remarkably, the relative elongation at the highest field (57.1 kA m^{-1}) was around 6.5 %. This elongation was higher than previously reported values for silicone elastomers of similar aspect ratio to our magnetic gels, which reached maximum elongations of around 4.5 % for much higher particle concentration (30 % v/v) and much stronger fields (approx. 1 T ≈800 kA/m) —see Fig. S5 [38]. Significantly, the magnetostriction of our gels was even higher than that reported for magnetic foams [39] (see Fig. S5), which due to the compressibility of the dispersed phase (*i.e.*, air) are *a priori* much more easily deformable.

The preparation and curing protocols had a significant impact on the magnetostriction behaviour of the magnetic gels. Significantly, the maximum magnetostriction became weaker when the gel was cured with the addition of $CaCl_2$ (*i.e.*, double calcium-curing) and thus, the degree of crosslinking was enhanced (Fig. 2b, S6-S8). Therefore, while double calcium-curing increased the solid-like, elastic, nature of the gels as shown in Fig. 1e, it did not improve the elongation upon field actuation. This result is not surprising though, because magnetostriction stems from a balance between the demagnetizing energy of the sample (which is reduced by elongation along the field) and its elastic energy (which increases with deformation), the latter being higher for more robust polymer networks under equal deformation. Similarly, pre-aligning the particles into elongated, chain-like, structures along the field direction during magnetic curing did not enhance the magnetostriction when compared to the simple calcium-cured samples, where the particles were isotropically distributed into clusters within the polymer matrix. This is an interesting result since, in general, anisotropic particle distribution is required for maximization of responsiveness to the field of magnetic elastomers and gels [7,29]. Our results can be explained by considering that particles isotropically distributed

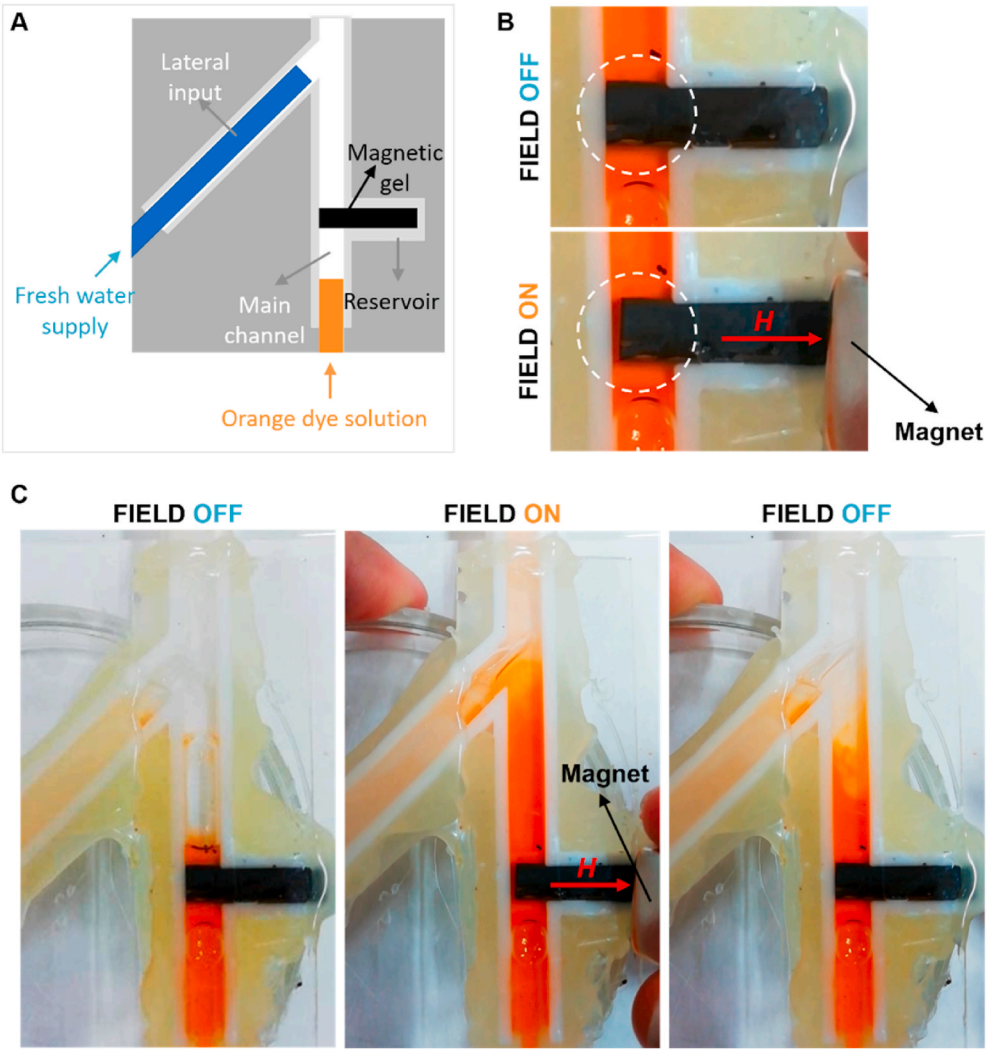

Fig. 4. Magnetically-actuated valve based on hydrogel length changes. **A.** Sketch of the magnetically-actuated valve. **B.** Snapshots showing hydrogel contraction in the direction perpendicular to the flow when a neodymium magnet was approached to the device. **C.** Snapshots from Supplementary Video 1 demonstrating the valve-like behaviour of the device. Brightness and contrast adjustments have been applied to the pictures in B and C. The direction of the applied magnetic field, *H*, is indicated with a red arrow. (For interpretation of the references to colour in this figure legend, the reader is referred to the Web version of this article.)

experience, in average, a higher magnetic field gradient when a field is applied than particles pre-aligned along the magnetic field, *i.e.*, already in the minimum energy configuration. Consequently, the internal magnetic forces giving rise to magnetostriction would have been higher for an isotropic distribution of particles, resulting in increased magnetostriction, in agreement with the results of Fig. 2b, S6-S8. Altogether, the data in Fig. 2b, S6-S8 suggest that although a certain degree of matrix rigidity is needed to enable magnetostriction (*i.e.*, liquid-like samples like suspensions do not experience magnetostriction), too tough hydrogel networks hinder it by reducing particle mobility and increasing the matrix elastic energy.

Changes in concentration of magnetic particles had different effects depending on the sample preparation method. For example, for the simple calcium-cured gel, raising the particle concentration from 2.5 % to 5 % v/v led to an increase of the field-induced elongation, when measured under the same strength of the magnetic field (Fig. 2b, S6-S8). Increasing the concentration of magnetic particles from 2.5 to 5 % also resulted in a slight decrease of the Young's modulus (Fig. 1e), and thus in a weaker polymer network, more deformable under an applied magnetic field. This, together with the stronger magnetic response associated with higher magnetic content, would explain the higher elongation of the 5 % sample. However, a further increase of the particle concentration from 5 % to 7.5 % v/v did not follow the same trend, and caused the maximum magnetostriction to decrease, although it remained higher than that of the 2.5 % sample. The same change in particle concentration gave rise to an increase of the Young's modulus, probably related to a larger number of particles connected by polymer strands. This increase of the stiffness of the 7.5 % v/v sample, could not, most likely, be compensated by the higher magnetic response associated with higher magnetic content, and thus, the deformability of the sample was hindered. Notably, for the double calcium-cured gels, the magnetostriction increased monotonically with the particle concentration (Fig. 2b, S6-S8), even though the stiffness of these gels also increased with the particle concentration, as evidenced by the increase of the Young's modulus observed in Fig. 1e. Therefore, in this case it seems most likely that the change of the magnetostriction with the particle concentration was less dependent on changes of the polymer network and should have been mostly ascribed to the enhancement of the magnetic response of the material upon field application. Finally, for the magnetic field-cured gels, increasing the particle concentration also resulted in stronger magnetostriction caused, again, by a more predominant effect of the magnetic interaction energy over the elastic one. Indeed, higher particle concentrations should result in thicker particle chain-like aggregates during magnetic curing, which in turn, should lead to increased magnetic forces.

We also monitored the length of the sample when the magnetic field was gradually removed, to get information on the reversibility of the field-induced elongation. As observed in Fig. 2a and summarised in Fig. 2c, samples did not fully recover the original dimensions immediately after field removal, thus demonstrating shape persistence and memory. In addition, for the same value of the magnetic field, the elongation was higher when the field was decreased after the maximum

field had been reached, *i.e.*, the downward curves (decreasing magnetic field) appeared above the upward curves (increasing magnetic field) in all cases (Fig. 2c). Therefore, the gels showed hysteretic behaviour, indicating that the relaxation of the elongation required longer times than those of our experiments. Indeed, after a time long enough from field removal no statistically significant differences in strain (deformation) were observed for gels subjected to magnetostriction experiments with respect to control gels (not subjected to magnetostriction, but only to gravity and time), as seen in Fig. S9. The normalized hysteresis area, quantified from plots like those in Fig. 2c, S6-S8, was in general higher for the double calcium-cured samples compared to the untreated gels —an exception was the sample with 5 % v/v particle concentration (Fig. 2d).

To get information on the responsiveness to the applied magnetic field over successive cycles of application/removal of the field, we subjected the hydrogels to fatigue experiments (Fig. S10). As observed, there was a gradual increase of strain for the successive cycles, both in the *on* state (under a magnetic field) and in the *off* state (after field removal). Interestingly, a significant responsiveness to the application/removal of the magnetic field was maintained in all cases over the total length of the experiments, more intense for the simple calcium-cured hydrogels at the highest magnetic field strength.

For magnetic field-cured gels, we also investigated the effect of the direction of the curing magnetic field on the magnetostriction (Fig. S11). As observed the magnetostriction was much higher when the sample was cured under a field at angles of 45° or 90° with respect to the direction of the field applied in magnetostriction experiments, highly likely because of the additional effect of the torque exerted by the magnetic field on particle chains inclined at an angle with respect to its direction. However, these samples (cured at angles of 45° or 90° with respect to field in magnetostriction experiments) did not maintain the cylindrical shape at the highest fields, suffering from bending, which for the particular case of 90° prevented from performing reliable measurements for fields above approx. 17 kA/m. On the contrary, the cylindrical shape remained stable in samples for which the curing field and magnetostriction field were parallel.

Concerning the increase in hysteresis area observed in Fig. 2d, this might be connected to a more robust polymer network obtained upon curing, which would lead to longer relaxation times. To corroborate this, we designed creep-recovery (*i.e.*, sudden deformation) experiments in which a constant stress (leading to deformations similar in magnitude to those in the magnetostriction experiments) was applied for 60 s with sample deformation (strain) monitoring, and then released while still recording the strain for 60 more seconds. As observed in Fig. S12 for samples with 7.5 % v/v particle concentration, the simple calcium-cured gels deformed almost instantaneously when the stress was applied, followed by an increase of the strain over time (Fig. S12a), a behaviour typical of a viscoelastic (Maxwell) liquid, in agreement with the low degree of crosslinking of these samples.

On the other hand, the strain measured for the double calcium-cured gels gradually increased with the applied stress (Fig. S12b), as it happens for a viscoelastic (Kelvin-Voigt) solid, associated with the strong crosslinking of the alginate matrix given by the calcium ions. Once the stress was released, the strain of the simple calcium-cured gels was very rapidly relaxed from *ca.* 5 %–1 % in a few seconds (Fig. S12a), while for the double calcium-cured gels, the decrease of strain was much more gradual (Fig. S12b).

To explain the remarkably high elongation of the simple calcium-cured gels at increasing magnetic fields, the microstructure of the gels was examined by optical and scanning electron microscopy (SEM). In agreement with previous results of our group [25], the magnetic particles appeared aggregated into particle clusters well integrated within the network of alginate fibres (Fig. 3a and b). The particle clusters presumably formed because at the sample preparation stage, the magnetic particles were added to an incipient gel matrix (*i.e.*, particles and the alginate gel were mixed after the gel had already reached some consistency, see Experimental section). In the case of the magnetic field-cured gels, the particle clusters had an elongated shape (Fig. 3a), corroborating the observations of Fig. 1b. We hypothesized that clustering of the particles would lead to a collective response responsible for the high magnetostriction of simple calcium-cured gels. Thus, based on these observations we developed a theoretical model for the magnetostriction (see Supplementary Information) that approximates the particle clusters as perfectly spherical inclusions of magnetic particles within the hydrogel environment (Fig. 3c). Under this approximation, and considering the whole sample as paramagnetic, we can estimate the total change in the free energy of the sample as the sum of the change associated to the interaction of the sample with the magnetic field and the change associated to the elastic contribution due to the deformation of the gel matrix. Then, by minimization of the change in free energy, we can obtain the equilibrium strain, ε, under a magnetic field, H, as:

$$\varepsilon = -\frac{\mu_0}{2}\frac{H^2}{(1+\chi_e N)^2 E}\left(\frac{d\delta\chi_e}{d\varepsilon} - \chi_e^2\frac{d\delta N}{d\varepsilon}\right). \quad \text{(S8)}$$

Here μ_0 is the vacuum magnetic permeability, χ_e is the effective (macroscopic) susceptibility of the sample, N is the demagnetizing shape-factor of the sample (δN, its change with the deformation), and $\delta\chi_e$ is the change of the susceptibility associated with changes in the relative positions of the paramagnetic inclusions because of the sample deformation. With the aim of fitting equation (S8) to the experimental data, we neglected $d\delta\chi_e/d\varepsilon$ vs. $\chi_e^2 d\delta N/d\varepsilon$, which should hold true since the susceptibility of the samples would have changed little for the experimental strains. We calculated the latter by using tabulated data for ellipsoids of revolution as in Ref. [40].

From equation (S8) ε is proportional to the square of the applied magnetic field, H^2. Thus, we plotted our experimental data against H^2 and fitted them to equation (S8) in Fig. 3d, using experimental values for the Young's modulus. According to the reduced chi-square statistics ($\chi^2 < 0.5$ in all cases), the experimental magnetostriction was well fitted by equation (S8) for the double calcium-cured gels (Fig. 3d, middle plot). For the simple calcium-cured gels (Fig. 3d, left plot), the fitting was reasonably good for low and high particle concentrations (*i.e.*, 2.5 and 7.5 v/v %; χ^2 in the range 0.6–1.7), but failed at the highest magnetic field strengths for medium particle concentrations (5 v/v %; $\chi^2 = 5.7$) and overestimated sample deformation (as discussed in the next paragraph). However, the fitting was poor for the gels cured under an external magnetic field ($\chi^2 > 3$) (Fig. S13), even at low magnetic fields. The most likely explanation in this latter case is that their magnetization would not follow a linear relationship with the magnetic field, because of the internal structuration of the magnetic particles into chains (as seen in Figs. 1a and 3a). To address this issue, we expanded our model to consider a non-linear relationship between the sample magnetization and the magnetic field (see Supplementary Information). In doing so, we obtained a more satisfactory fitting, as plotted in the right plot of Fig. 3d.

From the best fits we obtained the values of the sample susceptibility, and from these, the concentration of clusters in the ferrogels and the concentration of particles within the clusters, as shown in Table S1. As expected, raising the particle concentration from 2.5 to 7.5 % v/v led to an increase of the magnetic susceptibility, which in turn resulted in an almost proportional increase of the concentration of clusters. Significantly, the model seemed to predict a limit for the particle packing within the clusters, because increasing the particle concentration from 5 to 7.5 % v/v barely impacted the intra-cluster particle concentration, which remained ~10 % v/v. Remarkably, both the concentration of clusters and the particle concentration within these are qualitatively supported by our optical and electron microscopy observations [25]. Thus, our model quantitatively explains the monotonic increase of strain due to magnetostriction with particle concentration, as well as the dependence with the magnetic field for strongly crosslinked ferrogels (*i.e.*, double calcium-cured). For the simple calcium-cured gels, the experimental data are less well fitted at the highest magnetic fields for

the medium particle concentration (*i.e.*, 5 v/v %). Indeed, at the highest magnetic fields for this sample, a certain degree of saturation for the deformation was observed, although considerably less significant than for the gels cured under magnetic fields. A potential explanation is that the particle clusters might have displaced and changed their position from the position at zero field under a magnetic field. This is highly likely, given the weak crosslinking of the alginate network in these samples, and would explain why the magnetostriction gets saturated in a similar way to that of the gels cured under magnetic field, where particles were already aligned in the field direction prior to measurement. Indeed, we have previously demonstrated [41] that even for double calcium-cured gels, clusters of magnetic particles were able to move within the polymer network under much stronger fields (280 kA m^{-1}). This magnetic-field induced migration of particle clusters was also responsible of the strong MR effect developed by double calcium-cured alginate gels [41]. Following the same reasoning, the field-induced displacement and rearrangement of the particle clusters would have resulted in more complicated magnetostriction than this predicted by equation (S8). Therefore, we could conclude that the existence of clusters of magnetic particles, formed at the stage of sample preparation would be responsible for the large magnetostriction of our alginate gels. For weakly crosslinked gels (*i.e.*, simple calcium-cured), we might assume that displacement of clusters under an applied magnetic field would contribute to an additional enhancement of the magnetostriction of the composites.

We finally designed a proof-of-concept application with the aim of exploiting in soft actuator devices the responsiveness to magnetic fields of the magnetic hydrogels. We tested the performance of the gel in a valve. With this aim, we 3D-printed a device consisting of a main channel connected to a tube filled with an orange dye solution and provided with a reservoir for the magnetic gel (simple calcium-cured), Fig. 4a. In the absence of a magnetic field, the hydrogel blocked the channel as well as the flow of the dye solution, as shown in Fig. 4c. Downstream of the reservoir, the channel was provided with a side input which continuously supplied fresh water. When we placed a neodymium magnet close to the gel reservoir the magnetic gel contracted in the direction perpendicular to the flow, in response to the attraction towards the magnet provoked by the magnetic field gradient (Fig. 4b). Such contraction was large enough to allow the flow of the orange dye solution (Fig. 4c). As a result, the liquid at the outlet of the device was coloured in orange. Note that similarly to magnetostriction in a uniform field, the contraction here in the nonuniform field stems as a balance between the elasticity of the sample and its responsiveness to the field. When the magnet was removed, and thus the magnetic forces disappeared, the gel progressively elongated, recovering its original dimensions, thus, blocking completely the channel again approx. 2 s after field removal (Supplementary Video 1). This delay was due to the hysteretic behaviour of the hydrogel, which, as discussed above, was connected to the relaxation of the polymer network after deformation, and thus it could not be fully eliminated. Once the valve was closed again, and thanks to the continuous supply of fresh water by the side input, the liquid at the outlet of the tube became transparent again (Fig. 4c). The valve could be actuated several times without significant gel degradation. Although exploratory, our results suggest potential avenues for the design of soft actuators based on the almost unexplored magnetic hydrogels.

Supplementary video related to this article can be found at https://doi.org/10.1016/j.polymer.2021.124093

4. Conclusions

In conclusion, we have demonstrated that magnetic hydrogels prepared by dispersing magnetic particles within an incipiently formed matrix of alginate fibres largely change their length in response to an applied magnetic field. To quantify this responsiveness to the applied magnetic field, we have reported the magnetostriction (elongation during the process of magnetization) experienced by these samples. Remarkably high magnetostriction (*ca.* 6 %) is shown by gels with a low degree of network crosslink (simple calcium-cured gels), and thus, lower stiffness (Young's modulus). However, increasing the level of crosslinking of the alginate matrix by further addition of calcium ions (double calcium-cured gels) results in higher Young's modulus, which in turn restricts magnetostriction. Indeed, magnetostriction is an interplay between the elastic energy of the matrix and the magnetic energy of the sample, so stiffer matrices such as elastomers greatly oppose the field-induced deformation. When the constituent magnetic particles are pre-aligned during gelation into chain-like aggregates parallel to the magnetostriction field, the resulting samples do not experience strong magnetostriction either, because the gradient force felt by the particles in this case is smaller. Magnetostriction can be also modulated by varying the concentration of magnetic particles in the formulation, or the direction of the particle pre-alignment with respect to the direction of the field applied during magnetostriction. Remarkably, microscopic investigations of the gels show that the magnetic particles appear aggregated into clusters of irregular shape distributed along the alginate network for the gels cured in the absence of magnetic field, and into elongated clusters for the magnetic-cured gels. We have also demonstrated that these clusters are responsible for the strong magnetostriction of gels, because of the effective increase of the volume concentration of magnetic inclusions (clusters *vs*. individual particles) within the gels. Finally, we have developed a proof-of-concept application based on a valve bearing a magnetic gel remotely actuated by the magnetic field. Taken together, our results evidence the potential of magnetic hydrogels for applications in soft actuators, a field which has been traditionally dominated by magnetic elastomers. Compared to elastomers, magnetic gels also have the ability to largely change their mechanical properties (*e.g.*, their complex viscosity) with the magnetic field, closely behaving like magnetic suspensions, with the added advantage of negligible particle sedimentation. This dual behaviour, together with their biocompatible character, makes magnetic hydrogels excellent candidates for applications in a variety of fields including tissue engineering or soft robotics.

Data availability

All data is available in the main text or in the supplementary materials. Further details can be obtained from the corresponding author upon reasonable request.

CRediT authorship contribution statement

F.J. Vazquez-Perez: Conceptualization, Formal analysis, Investigation, Validation, Visualization. **C. Gila-Vilchez:** Formal analysis, Investigation, Validation. **J.D.G. Duran:** Conceptualization, Funding acquisition, Supervision. **A. Zubarev:** Formal analysis, Methodology, Writing – original draft. **L. Alvarez de Cienfuegos:** Conceptualization, Funding acquisition, Writing – review & editing. **L. Rodriguez-Arco:** Conceptualization, Visualization, Writing – original draft, Writing – review & editing. **M.T. Lopez-Lopez:** Conceptualization, Funding acquisition, Methodology, Project administration, Supervision, Writing – original draft, Writing – review & editing.

Declaration of competing interest

The authors declare that they have no known competing financial interests or personal relationships that could have appeared to influence the work reported in this paper.

Acknowledgements

Dr. Mariusz Barczak is acknowledged for help with SEM imaging of iron particles. Ms. Laura Quesada de la Torre is acknowledged for help

with design of graphical abstract. This study was supported by project FIS2017-85954-R (Ministerio de Economía, Industria y Competitividad, MINECO, and Agencia Estatal de Investigación, AEI, Spain, cofunded by Fondo Europeo de Desarrollo Regional, FEDER, European Union). CGV acknowledges financial support by Ministerio de Ciencia, Innovación y Universidades and University of Granada, Spain, for her FPU17/00491 grant. AZ thanks the Russian Science Foundation, project 20-12-00031, for the financial support. LRA thanks the Spanish State Research Agency (Spanish Ministry of Science and Innovation) through Juan de la Cierva Incorporacion Fellowship (IJC2018-037951-I). Funding for open access charge: Universidad de Granada / CBUA.

Appendix A. Supplementary data

Supplementary data to this article can be found online at https://doi.org/10.1016/j.polymer.2021.124093.

References

[1] O. Erol, A. Pantula W. Liu, D.H. Gracias, Adv. Mater. Technol. 4 (2019), 1900043, https://doi.org/10.1002/admt.201900043.
[2] J.A.C. Liu, J.H. Gillen, S.R. Mishra, B.A. Evans, J.B. Tracy, Sci. Adv. 5 (2019), eaaw2897, https://doi.org/10.1126/sciadv.aaw2897.
[3] O. Ranunkel, F. Güder, ACS Appl. Bio Mater. 2 (2019) 1490–1497, https://doi.org/10.1021/acsabm.8b00753.
[4] H. Ding, X. Liang, S.Y. Zheng, Q. Wang, Z. Li, G. Sun, Mater. Chem. Phys. 253 (2020), 123332, https://doi.org/10.1016/j.matchemphys.2020.123332.
[5] M.-Y. Choi, Y. Shin, H.S. Lee, S.Y. Kim, J.-H. Na, Sci. Rep. 10 (2020) 2482, https://doi.org/10.1038/s41598-020-59318-3.
[6] Z. Feng, H. Zuo, J. Hu, W. Gao, B. Yu, N. Ning, M. Tian, L. Zhang, Ind. Eng. Chem. Res. 59 (2020) 166–174, https://doi.org/10.1021/acs.iecr.9b04521.
[7] S.R. Goudu, I.C. Yasa, X. Hu, H. Ceylan, W. Hu, M. Sitti, Adv. Funct. Mater. 30 (2020), 2004975, https://doi.org/10.1002/adfm.202004975.
[8] X. Liu, J. Liu, S. Lin, X. Zhao, Mater. Today 36 (2020) 102–124, https://doi.org/10.1016/j.mattod.2019.12.026.
[9] Y. Lee, W.J. Song, J.-Y. Sun, Mater. Today Phys. 15 (2020), 100258, https://doi.org/10.1016/j.mtphys.2020.100258.
[10] K.Y. Lee, D.J. Mooney, Chem. Rev. 101 (2001) 1869–1880, https://doi.org/10.1021/cr000108x.
[11] J. Li, D.J. Mooney, *Nat. Rev*. Mater. 1 (2016) 16071, https://doi.org/10.1038/natrevmats.2016.71.
[12] H. Banerjee, M. Sudhail, H. Ren, Biomimetics 3 (2018) 15, https://doi.org/10.3390/biomimetics3030015.
[13] S. Talebian, M. Mehrali, N. Taebnia, C.P. Pennisi, F.B. Kadumudi, J. Foroughi, M. Hasany, M. Nikkhah, M. Akbari, G. Orive, A. Dolatshahi-Pirouz, Adv. Sci. 6 (2019), 1801664, https://doi.org/10.1002/advs.201801664.
[14] J.M. Korde, B. Kandasurbramanian, Chem. Eng. J. 379 (2020), 122430, https://doi.org/10.1016/j.cej.2019.122430.
[15] S. Fuchs, K. Shariati, M. Ma, Adv. Healthcare Mater. 9 (2020), 1901396, https://doi.org/10.1002/adhm.201901396.
[16] W. Shi, J. Huang, R. Fang, M. Liu, *ACS* Appl. Mater. Interfaces 12 (2020) 5177–5194, https://doi.org/10.1021/acsami.9b16770.
[17] R. Tognato, A.R. Armiento, V. Bonfrante, R. Levato, J. Malda, M. Alini, D. Englin, G. Giancane, T. Serra, Adv. Funct. Mater. 29 (2019), 1804647, https://doi.org/10.1002/adfm.201804647.
[18] J. Tang, C. Yao, Z. Gu, S. Jung, D. Luo, D. Yang, Angew. Chem. Int. Ed. 59 (2020) 2490–2495, https://doi.org/10.1002/anie.201913549.
[19] J. Tang, Q. Yin, Y. Qiao, T. Wang, ACS Appl. Mater. Interfaces 11 (23) (2019) 21194–21200, https://doi.org/10.1021/acsami.9b05742.
[20] B.P. Nowak, B.J. Ravoo, Farady Discuss 219 (2019) 220, https://doi.org/10.1039/c9fd00012g.
[21] M. Li, Y. Wang, A. Chen, A. Naidu, B.S. Napier, W. Li, C. Lopez-Rodriguez, S. A. Crooker, F.G. Omenetto, Proc. Natl. Acad. Sci. Unit. States Am. 115 (32) (2018) 8119–8124, https://doi.org/10.1073/pnas.1805832115.
[22] J.C. Breger, C. Yoon, R. Xiao, H.R. Kwang, M.O. Wang, J.P. Fisher, T.D. Nguyen, D. H. Gracias, ACS Appl. Mater. Interfaces 7 (5) (2015) 3398–3405, https://doi.org/10.1021/am508621s.
[23] J. Thévenot, H. Oliveira, O. Sandre, S. Lecommandoux, Chem. Soc. Rev. 42 (2013) 7099, https://doi.org/10.1039/c3cs60058k.
[24] R. Contreras-Montoya, A.B. Bonhome-Espinosa, A. Orte, D. Miguel, J.M. Delgado-López, J.D.G. Duran, J.M. Cuerva, M.T. Lopez-Lopez, L. Alvarez de Cienfuegos, Mater. Chem. Front. 2 (2018) 686–699, https://doi.org/10.1039/c7qm00573c.
[25] C. Gila Vilchez, A.B. Bonhome-Espinosa, P. Kuzhhir, A. Zubarev, J.D.G. Duran, M. T. Lopez-Lopez, J. Rheol. 62 (2018) 1083–1096, https://doi.org/10.1122/1.5028137.
[26] H. Böse, Int. J. Mod. Phys. B 21 (2007) 4790–4797, https://doi.org/10.1142/S0217979207045670.
[27] H. Böse, R. Röder, J. Phys. Conf. Ser. 149 (2009), 012090, https://doi.org/10.1088/1742-6596/149/1/012090.
[28] M.N.H. Hadzir, M.H.A. Bakar, A.I. Azis, Effect of the magnetic field on magnetic particles in magnetorheological elastomer layers, in: A. Ismail, M.H. Abu Bakar, A. Öchsner (Eds.), Advanced Engineering for Processes and Technologies, Springer, New York, NY, 2019, pp. 135–143, 2019.
[29] S.R. Mishra, M.D. Dickey, O.D. Velev, J.B. Tracy, Nanoscale 8 (2016) 1309–1313, https://doi.org/10.1039/C5NR07410J.
[30] A.P. Safronov, E.A. Mikhnevich, J. Phys. Conf. Ser. 1389 (2019), 012057, https://doi.org/10.1088/1742-6596/1389/1/012057.
[31] J. Sun, H. Tan, Materials 6 (2013) 1285–1309, https://doi.org/10.3390/ma6041285.
[32] M. Barczak, P. Borowski, C. Gila-Vilchez, M. Alaminos, F. Gonzalez-Caballero, M. T. Lopez-Lopez, Carbohydr. Polym. 247 (2020) 116747, https://doi.org/10.1016/j.carbpol.2020.116747.
[33] F. Campos, A.B. Bonhome-Espinosa, R. Carmona, J.D. Duran, P. Kuzhir, M. Alaminos, M.T. Lopez-Lopez, I.A. Rodriguez, V. Carriel, Mater. Sci. Eng. C 118 (2021), 111476, https://doi.org/10.1016/j.msec.2020.111476.
[34] L. Rodriguez-Arco, I.A. Rodriguez, V. Carriel, A.B. Bonhome- Espinosa, F. Campos, P. Kuzhir, J.D.G. Duran, M.T. Lopez-Lopez, Nanoscale 8 (2016) 8138–8150, https://doi.org/10.1039/c6nr00224b.
[35] R.K. Singh, K.D. Patel, J.H. Lee, E.-J. Lee, J.-H. Kim, T.-H. Kim, H.-W. Kim, PloS One 9 (2014), e91584, https://doi.org/10.1371/journal.pone.0091584.
[36] S. Hao, J. Meng, Y. Zhang, J. Liu, X. Nie, F. Wu, Y. Yang, C. Wang, N. Gu, H. Xu, Biomaterials 140 (2017) 16–25, https://doi.org/10.1016/j.biomaterials.2017.06.013.
[37] T.F. Anderson, Trans. N. Y. Acad. Sci. 13 (1951) 130–133, https://doi.org/10.1111/j.2164-0947.1951.tb01007.x.
[38] G. Diguet, E. Beaugnon, J.Y. Cavaillé, J. Magn. Magn Mater. 332 (21) (2010) 3337–3341, https://doi.org/10.1016/j.jmmm.2010.06.020.
[39] Y. Wang, G. Guo, Y. Zhou, Y. Sun, D. Li, Y. Liu, G. Zhao, Compos. Sci. Technol. 170 (2019) 34–41, https://doi.org/10.1016/j.compscitech.2018.11.023.
[40] A.Y. Zubarev, D.Y. Borin, J. Magn. Magn Mater. 377 (2015) 373–377, https://doi.org/10.1016/j.jmmm.2014.10.141.
[41] C. Gila-Vilchez, J.D.G. Duran, F. Gonzalez-Caballero, A. Zubarev, M.T. Lopez-Lopez, Smart Mater. Struct. 28 (2019), https://doi.org/10.1088/1361-665X/aafeac, 035018.
[42] J.E. Martin, R.A. Anderson, Electrostriction in field-structured composites: Basis for a fast artificial muscle? J. Chem. Phys. 111 (1999) 4273–4280, https://doi.org/10.1063/1.479725.
[43] S.M. Mirvakili, I.W. Hunter, Artificial muscles: mechanisms, applications, and challenges, Adv. Mater. 30 (2018), 1704407, https://doi.org/10.1002/adma.201704407.
[44] H. Böse, R. Rabindranath, J. Ehrlich, Soft magnetorheological elastomers as new actuators for valves, J. Intell. Mater. Syst. Struct. 23 (2011) 989–994, https://doi.org/10.1177/1045389X11433498.
[45] S.R. Sershen, G.A. Mensing, M. Ng, N.J. Halas, D.J. Beebe, J.L. West, Independent optical control of microfluidic valves formed from optomechanically responsive nanocomposite hydrogels, Adv. Mater. 17 (2005) 1366–1368, https://doi.org/10.1002/adma.200401239.
[46] A.D.M. Charles, A.N. Rider, S.A. Brown, C.H. Wang, Multifunctional magneto-polymer matrix composites for electromagnetic interference suppression, sensors and actuators, Prog. Mater. Sci. 115 (2021), 100705, https://doi.org/10.1016/j.pmatsci.2020.100705.